ACTIVE NOISE CONTROL IN ENCLOSED SPACES

Jignan Guo and Murray Hodgson
Occupational Hygiene Programme and Department of Mechanical Engineering,
University of British Columbia, Vancouver, B.C., Canada V6T 1Z4

Introduction

Much of the progress on active noise control (ANC) has been achieved in the case of one-dimensional sound-fields, as found in ducts or very small enclosed spaces, such as hearing protectors. The possibility of using ANC to attenuate noise in free-field environments has been studied. ANC in three-dimensional enclosed sound fields, such as rooms and aircraft cabins, though relatively difficult, has also attracted increased studies. though the special cases of a low modal density[1-4] or a diffuse sound field[5-10] are always assumed. When the enclosed space is very small (that is, the wavelength at the frequency of interest is large compared with its size), the sound field consists of a few dominant modes, and the modal-depression method is often used. The sound energy can be significantly attenuated by reducing the energy of each mode. This is the mechanism normally involved in active air-mufflers and active noise control in small cabins. However, when the enclosure is large (that is, the wavelength at the frequency of interest is much smaller than its size), there are too many modes to be controlled. An approach that assumes that the enclosure contains a diffuse sound field demonstrates that the noise can be controlled only over a very small area. However, in many practical enclosed environments, the sound field is neither of low modal density nor diffuse - examples are workshops, offices, and classrooms[11]. The noise in these environments is usually difficult, or even impossible, to control by traditional means. The application of ANC in such non-diffuse environments is an option that needs to be investigated theoretically, and with respect to practical implementation.

In this paper, the effectiveness of ANC in enclosed environment is studied using an image-source model developed in this study. Both global and local control strategies are investigated with different configurations of the primary source, control source and error microphone. The total power output of the sources, and the size of quiet zone created by the local control strategy, are the two indicators of control efficiency used in this study.[12]

Image-source model

To calculate the effectiveness of ANC in an enclosure, a sound prediction model is necessary. There are many such models based on ray-tracing, image-source, and modal analysis. However, most of the existing models are either too time-consuming, or are unable to provide phase information that necessary for ANC analysis.

A computer model based on the image-source approach has been developed for the general analysis of ANC in enclosed spaces. According to the image-source method, for a rectangular enclosure, the steady-state sound pressure at a position X generated by a point sound source located at X' can be expressed by[13]

$$p(X,X') = qA\sum_{p=0}^{1}\sum_{r=-\infty}^{\infty}\beta_{x1}^{|n-q|}\beta_{x2}^{|n|}\beta_{y1}^{|l-j|}\beta_{y2}^{|l|}\beta_{z1}^{|m-s|}\beta_{z2}^{|m|}\frac{e^{-ik|R_p+R_r|}}{|R_p+R_r|}$$

Theoretically, an infinite number of reflections from the walls (infinite image sources) needs to be included in the calculation. However, this is impossible in practice. One of the main tasks of the model development was to determine the least number of images that is accurate enough to describe the sound field. It has been found in this study that the least number of images depends on many room parameters, such as the room dimension, reflection coefficients of the walls, and the location of the sound source. Figure 1 shows how the calculated sound power output of the source W changes with increased number of images included N. The enclosure in this example is a rectangular room with dimension of 15×20×6 m^3. The reflection coefficients of the six walls are chosen to be the same, and to take the values B indicated.

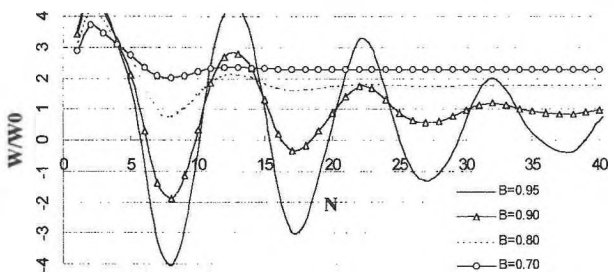

Fig. 1. Power output via the number of images.

It can be shown that the calculated sound-power output gradually converges with the increase of the reflections included. The lower are the reflection coefficients of the walls, the less is the number of the images needs to be calculated. In the example above, more than 40 reflections needed to be included when the reflection coefficient is B=0.90. This number reduced to 21 and 12 when the reflection coefficient decreased to 0.80 and 0.70, respectively.

Sound energy reduction

The reduction of total sound energy in the enclosure was studied through the reduction of total sound-power output when a control source was introduced into the enclosure, using the image-source model. The power-output reduction in a room considered by Bullmore et al.[2] which is of the dimensions of 2.264×1.132×0.186 m^3 is shown in Fig. 2 for both global and local control strategies. The primary source is at (0,0,0), the control source at (2.264,0,0), and the error microphone at (1.132,0.566,0) for local control. The reflection coefficients of all six walls were chosen to be the same at B=0.9. It shows that both global and local control strategies reduce the sound energy in the enclosure significantly at low frequencies (f<120 Hz). At high frequencies, while the local-control strategy increases the sound energy, the global-control strategy is still effective in some frequency ranges.

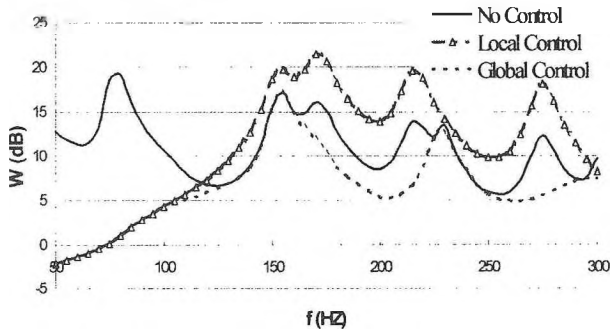

Fig. 2. Total energy reductions with both control strategies.

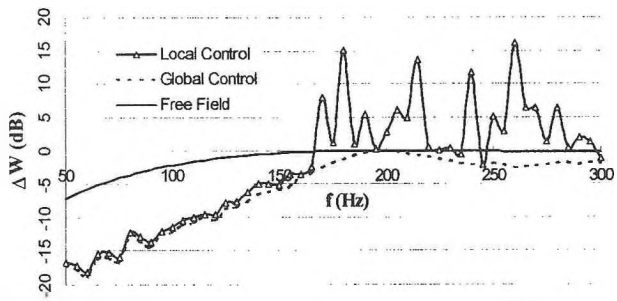

Fig. 3. Energy reduction with primary source at (0,0,0).

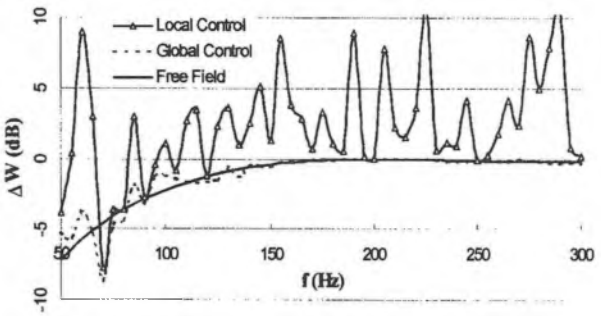

Fig. 4. Energy reduction with primary source at (7.5,10,3).

However, it has been found in this study that the performance of the control system depends not only on the relative position of the primary and control sources, but also on their positions in the enclosure. A rectangular room with dimensions of 15×20×6 m^3 is chosen to illustrate this fact. Figure 3 shows the total sound-power output reduction for both global and local control strategies. The global reduction in free-space is also included as a reference. The primary source is at (0,0,0), the control source is at (0.5,0.5,0.5), and the error microphone is at (7.5,10,3). The reflection coefficients of the walls have the same value of B=0.90, and 41 reflections are included in the calculation. A significant total sound-power output reduction is seen for both control strategies at low frequencies (f<150 Hz), and the reduction in the enclosure is much larger than that in free-space for the same separation of the primary and control sources. Figure 3 also implies that the local control strategy works as well as global control strategy does in achieving big reduction of sound energy at low frequencies, which is much easier to be implemented.

When the primary source is at (7.5,10,3), and the control source is at (8,10.5,3.5) and the error microphone is at (15,20,6), the power-output reduction at low frequencies for both control strategies decreases, as shown in Fig. 4. The difference between the results of Fig. 3 and Fig.4 are very evident at low frequencies, even though the distance between the primary and control sources is the same in these two configurations.

More analysis indicates that, in most cases, the sound-energy reduction is more significant for both control strategies when the primary source is in a corner or close to a wall of the enclosure.

Sound-pressure reduction

The same enclosure of 15×20×6 m^3 with the same reflection coefficients of the six walls, B=0.90, is chosen to demonstrate the sound-pressure reduction. Figure 5 shows the sound-pressure reduction in the enclosure by the global-control strategy when the primary source is at (0,0,0), the control source is at (0.5,0.5,0.5), and the error microphone is at (7.5,10,3). A sharp reduction of sound pressure (more than 10 dB) occurs almost everywhere within the enclosure. The reduction by the local control strategy in this case is very similar.

However, the large reduction of sound pressure in the whole enclosure disappears when the primary source is located at (7.5,10,3) when the local-control strategy is applied, as shown in

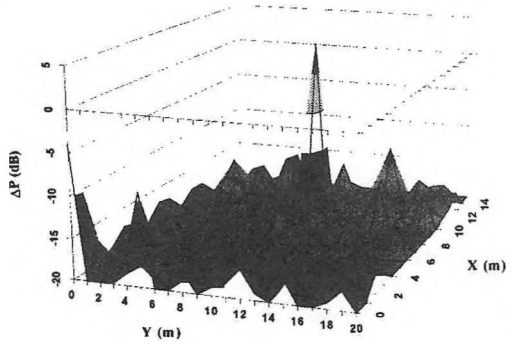

Fig. 5. Pressure reduction with primary source at (0,0,0).

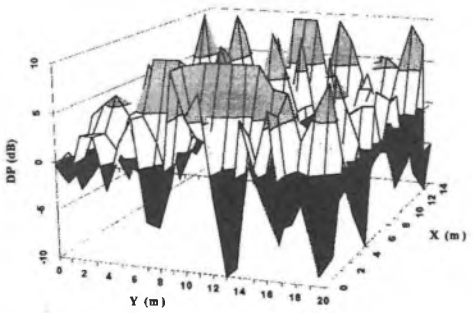

Fig. 6. Pressure reduction with primary source at (7.5,10,3).

Fig. 6, even when the separation of the primary and control sources is the same as in the case shown in Fig. 5. The control source makes the sound field very non-uniform in this case. It reduces sound pressure at some places, but increases it in other places. No large quiet zones exists.

It has been found in this study that the size of the quiet zone created around the error microphone is also dependent on the positions of the sources and error microphone, as well as the frequency of interest and the reflection coefficients of the walls. Figure 7 shows the size of the quiet zone created by the control system when the primary source is at (7.5,0,3), the control source is at (7.5,10,3), and the error microphone is at (7.5,15,3). It is obvious that the size of the quiet zone is much larger than an area with maximum diameter of λ/10, a typical size of the quiet zone predicted in a diffuse field.

Conclusions

The image-source model works well in the analysis of ANC in enclosures, and can accurately describe the sound field with not many images when the reflection coefficients of the walls are not very large.

The total sound energy can be greatly reduced, or a large quiet zone can be created in the enclosure when the control system is suitably arranged. However, the control efficiency is highly dependent, not only on the relative positions of the primary and control sources, but also on the positions of the sources and error microphone in the enclosure. There are preferable locations for the primary source for which the control system works much better.

References

1. P.A. Nelson *et al.*, J. Sound and Vib., **117** (1), 1-13 (1987).
2. A.J. Bullmore *et al.*, J. Sound and Vib., **117** (1), 15-33 (1987).
3. M. Tohyama & A. Suzuki, J. Sound and Vib., **119** (3), 562-564 (1987).
4. C. Bao *et al.*, J. Sound and Vib., **161** (3), 501-514 (1993).
5. A. David & S.J. Elliott, Applied Acoustics, **41**, 63-79 (1994).
6. P. Joseph *et al.*, J. Sound and Vib., **172** (5), 605-627 (1994).
7. P. Joseph *et al.*, J. Sound and Vib., **172** (5), 629-655 (1994).
8. J. Elliott and J. Garcia-Bonito, J. Sound and Vib., **186**(4), 696-704 (1995).
9. J. Garcia-Bonito and S. J. Elliott, ***ISVR Technical Memorandum* 745** (1994).
10. J. Garcia-Bonito & S.J. Elliott, J. Acoust. Soc. Am., **98** (2), 1017-1204 (1995).
11. Murray Hodgson, Applied Acoustics, **49**, 197-207 (1996).
12. Jingnan Guo *et al.*, J. Acoust. Soc. Am. **101** (3), 1492-1501 (1997).
13. J.B. Allen & D.A. Berkley, J. Acoust. Soc. Am., **65** (4), 943-950 (1995).

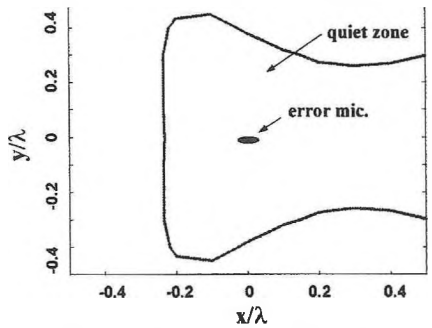

Fig. 7. Quiet zone around error microphone.